Plant, Cell & Environment

*Plant, Cell and Environment* (2016) **39**, 694–705 doi: 10.1111/pce.12668

## Original Article

# Stomatal dynamics are limited by leaf hydraulics in ferns and conifers: results from simultaneous measurements of liquid and vapour fluxes in leaves

Samuel C. V. Martins[1,2], Scott A. M. McAdam[1], Ross M. Deans[1], Fábio M. DaMatta[2] & Tim J. Brodribb[1]

*[1]School of Biological Sciences, University of Tasmania, Private Bag 55, Hobart, Tasmania 7001, Australia and [2]Departamento de Biologia Vegetal, Universidade Federal de Viçosa, 36570-000, Viçosa, MG, Brazil*

## ABSTRACT

**Stomatal responsiveness to vapour pressure deficit (VPD) results in continuous regulation of daytime gas-exchange directly influencing leaf water status and carbon gain. Current models can reasonably predict steady-state stomatal conductance ($g_s$) to changes in VPD but the $g_s$ dynamics between steady-states are poorly known. Here, we used a diverse sample of conifers and ferns to show that leaf hydraulic architecture, in particular leaf capacitance, has a major role in determining the $g_s$ response time to perturbations in VPD. By using simultaneous measurements of liquid and vapour fluxes into and out of leaves, the *in situ* fluctuations in leaf water balance were calculated and appeared to be closely tracked by changes in $g_s$ thus supporting a passive model of stomatal control. Indeed, good agreement was found between observed and predicted $g_s$ when using a hydropassive model based on hydraulic traits. We contend that a simple passive hydraulic control of stomata in response to changes in leaf water status provides for efficient stomatal responses to VPD in ferns and conifers, leading to closure rates as fast or faster than those seen in most angiosperms.**

*Key-words*: Leaf capacitance; leaf hydraulic conductance; leaf water content; stomatal conductance; vapour pressure deficit.

## INTRODUCTION

Efficiency in resource use appears as a central theme in the evolution and function of the vegetative plant body (McAdam & Brodribb 2012a). Probably the most dynamic example of this behaviour is the management of water use by stomatal valves on the leaf surface. Stomata respond rapidly to changes in evaporative demand (e.g. vapour pressure and temperature) or photosynthetic potential (e.g. light intensity and $CO_2$ partial pressure) by regulating the size of the pore to maintain an optimum balance between evaporation and photosynthesis (Cowan & Farquhar 1977). These stomatal movements are ubiquitous among plant species and profoundly affect diurnal and seasonal trends in water and carbon movement between plants and the atmosphere (Farquhar *et al*. 1993; Hetherington & Woodward 2003). The importance of incorporating stomatal behaviour into global circulation models has been recently recognized (Cramer *et al*. 2001; Barman *et al*. 2014), but there remains considerable debate about the mechanisms that drive stomatal movements, undermining the predictive capacity of these models (Damour *et al*. 2010).

In hydrated plants, stomatal responses to changes in evaporative demand [or the vapour pressure difference between leaves and the atmosphere: vapour pressure deficit (VPD)] result in continuous regulation of daytime gas exchange over the timescale of seconds to minutes (Sellin & Lubenets 2010). Hydraulic models of water balance in the leaf are able to reasonably predict steady-state stomatal conductance in response to changes in VPD (Tyree & Sperry, 1988; Oren *et al*. 1999), but there has been little research into the dynamic behaviour of stomata between these steady-states. This is a potentially important knowledge gap because the kinetics of a stomatal response to changes in VPD may vary considerably between species and strongly influence the efficiency of water use by plants. Just as slow stomatal responses to changing light intensity lead to suboptimal diurnal ratios of leaf transpiration ($E$) over net photosynthesis ($A$) (Lawson & Blatt 2014), a species responding slowly to changes in VPD will be less efficient in maintaining an optimal diurnal ratio of $\partial E/\partial A$ in relation to stomatal conductance ($g_s$) than species with faster-responding stomata (Buckley 2005).

A major limitation to predicting how leaves should respond to VPD is uncertainty about the mechanism driving changes in guard cell turgor (Damour *et al*. 2010). At one end of a hypothetical spectrum, hydropassive stomatal control predicts stomatal aperture directly as a function of changing leaf hydration during a VPD transition (Lange *et al*. 1971; Brodribb & McAdam 2011; Peak & Mott 2011), while at the other extreme, VPD is thought to influence levels of the phytohormone abscisic acid (ABA), which regulates an active process of guard cell turgor control (Bauer *et al*. 2013, McAdam & Brodribb, 2015). Illuminating this debate is evidence of an evolutionary transition from an ancestral hydropassive stomatal behaviour in ferns and lycophytes and a derived ABA-dependent control of stomatal responses to VPD in angiosperms (Brodribb & McAdam 2011; McAdam & Brodribb

*Correspondence: T. J. Brodribb. e-mail: timothyb@utas.edu.au*

2015). The predicted kinetics of a stomatal response to VPD, if guard cells were uniquely controlled by ABA, would depend on a number of unknown factors such as the rate of ABA synthesis, catabolism and signalling (Kim *et al.* 2010) and would more than likely result in pronounced hysteresis (McAdam & Brodribb, 2015). On the other hand, if the stomata respond passively to leaf hydration, then the response time after a change in VPD would depend on the balance of the physical properties of the leaf including hydraulic conductance, capacitance and evaporation, and would only produce hysteresis if hydraulic conductance changed in response to evaporation (Simonin *et al.* 2014). A tight association between plant hydraulic characteristics and stomatal behaviour in response to water stress has been seen in ferns and lycophytes, consistent with passive stomatal behaviour in these lineages, but the response of conifers suggests that both ABA and hydropassive influences are important (McAdam & Brodribb 2013, 2014).

The first step towards understanding the kinetics of stomatal responses to VPD transitions must be to understand how leaf water potential ($\Psi_w$) changes during perturbations in leaf transpiration. This type of 'real-time' measure of $\Psi_w$ is typically impossible because of the fact that $\Psi_w$ must be measured destructively in a pressure chamber or under very stable conditions using a leaf psychrometer. Here, we employ a new technique to calculate $\Psi_w$ dynamically, based upon the measured balance between liquid and vapour fluxes into and out of the leaf (the dual flux technique). This technique allowed us to examine whether stomatal kinetics in fern and conifer species conform to the expectations of a hydropassive control during step changes in VPD. Additionally, it was also possible to estimate the response of leaf hydraulic conductance ($K_L$) to VPD in a non-destructive manner, which is of extreme importance considering recent reports suggesting a highly dynamic nature of $K_L$ (Prado & Maurel, 2013; Simonin *et al.* 2014). Furthermore, we employed the dual flux technique to examine the importance of hydraulic parameters in determining the speed of stomatal responses to VPD. If hydropassive control is the dominant mechanism, the speed of the response will be dictated by the balance between dynamic capacitance ($C_{dyn}$) and $K_L$, whereas the magnitude will be dependent on the relationship between guard cell turgor pressure and $\Psi_w$. If stomata are controlled by ABA levels, then different rates of synthesis, signalling and ABA catabolism would dominate the kinetics of the stomatal response and hysteresis would be expected.

## MATERIAL AND METHODS

### Plant material and experimental conditions

Four fern species and two conifers (one deciduous and one evergreen) were selected as examples of diverse species known to be suitable for excision studies (lacking mucilage or resin canals close to the xylem). Potted individuals of the fern species *Adiantum capillus-veneris* L., *Cheilanthes myriophylla* Desv., *Hypolepis tenuifolia* (G. Forst.) Bernh., *Pyrrosia lingua* (Thunb.) Farw. and the conifers *Metasequoia glyptostroboides* Hu and W. C. Cheng and *Callitris rhomboidea* R.Br ex Rich. & A. Rich were used in this study. Plants were grown in the glasshouses of the School of Biological Sciences, University of Tasmania, Hobart, Australia under controlled conditions of 25 °C/16 °C day/night temperatures and 16 h photoperiod, with natural light supplemented by sodium vapour lamps to ensure a minimum 300 $\mu$mol quanta $m^{-2} s^{-1}$ at the pot surface. All plants received weekly applications of liquid fertilizer (Aquasol, Hortico Ltd), and measurements were undertaken from February to April, 2014.

### Stomatal size

Mean guard cell length in each species was measured from three leaves (one leaf per individual, $n = 20$ stomata per leaf). Epidermal preparations were made by soaking leaf samples in commercial bleach (50 g $L^{-1}$ sodium hypochlorite and 13 g $L^{-1}$ sodium hydroxide) for 24–48 h until the epidermis separated from the mesophyll and could be washed and viewed and photographed at 40× magnification using Differential Interference Contrast (DIC) with a Leica DFC450 digital microscope camera mounted on a Leica DM 2000 (Nussloch, Germany).

### $C_{dyn}$ determined by bulk flow

Leaf capacitance was measured directly on four leaves from each species (one leaf per individual) by calculating the bulk volume of water absorbed by a leaf or shoot hydrating from a mild water potential (approximately −0.5 to −1 MPa) while connected to a flowmeter (Blackman & Brodribb 2011; Brodribb & Blackman 2011). Here, leaf capacitance was calculated as the volume of water taken up by the leaf during a transition from an initial $\Psi_w$ ($\Psi_o$) to a final $\Psi_w$ ($\Psi_f$):

$$C_{dyn} = \sum F / (\Psi_o - \Psi_f) \quad (1)$$

where $\sum F$ is the sum of the flow of water into the leaf during rehydration adjusted for leaf area (mmol $m^{-2}$) and temperature following Brodribb & Holbrook (2006). Importantly, initial maximum flow ($F$) in these rehydration plots was determined by fitting an exponential curve through the first 20 s of the rehydration flow data and extrapolating back to the initial point of leaf excision, taking into account the 2–3 s required to connect the sample to the flowmeter. Over this initial 20 s period, a single parameter exponential curve always provided a good fit to the data ($r^2 > 0.95$).

### Liquid and vapour flux measurements

Leaf gas exchange in three to four even-aged leaves (one leaf per individual) was measured using an infrared gas analyser (LI-6400, LI-COR Biosciences) equipped with a conifer chamber (6400–05, LI-COR Biosciences), and liquid flow was simultaneously measured with a custom-built

flowmeter (for construction details, see Brodribb & Blackman 2011). First, leaves were excised under degassed resin-filtered, deionized water, connected to a flowmeter and then fully enclosed in the chamber. Irradiance was provided by a fibre-optic light source, providing a minimum light intensity of 300 $\mu$mol quanta $m^{-2} s^{-1}$ at the leaf surface, which was very near the light intensity required for saturating $g_s$. Conditions in the chamber were controlled at a block temperature of 22 °C, leaf temperature was measured with a thermocouple connected to a datalogger (CR1000, Campbell Scientific Inc.) and VPD was regulated by a portable dew point generator (LI-610, LI-COR Biosciences). Upon enclosure in the cuvette, initial VPD was set at $1.0 \pm 0.1$ kPa, and instantaneous gas exchange and liquid flux were logged every 10 s. After $g_s$ reached stability (approximately 15 min), VPD was increased to $2.2 \pm 0.3$ kPa and maintained until liquid and vapour fluxes were matched and/or $g_s$ was stable (approximately 10 min). Afterwards, VPD was lowered back to initial conditions and maintained until $g_s$ stability was re-established. Then, leaves were removed from the chamber and flowmeter, immediately wrapped in damp paper towel, and bagged for 10 min to allow tissue equilibration prior to $\Psi_w$ measurement. Final $\Psi_w$ was measured using a Scholander pressure chamber and microscope to precisely measure xylem balance pressure. VPD was increased instantly by passing the incoming air through a desiccant column (such a treatment was faster than changing VPD using the dew point generator). In the same way, VPD was decreased by bypassing the desiccant column, returning the incoming air source directly to the dew point generator. Because of differences in equilibration time between the reference and sample infrared gas analysers (IRGAs), data from the first two minutes immediately after the VPD transition were discarded. Then, this gap was filled by fitting a model of an exponential decay through the remaining observed $g_s$ data (under high or low VPD) and extrapolating back to the initial point where $g_s$ started to decrease (transition to high VPD) or increase (transition to low VPD) (Supporting Information Fig. S1). Such a procedure was feasible because ferns and conifers do not have hydropassive, wrong-way responses as they lack an epidermal mechanical advantage (Franks & Farquhar 2007; Brodribb & McAdam 2011; McAdam & Brodribb 2012b).

## Leaf water potential and hydraulic conductance reconstructions

The rate of change in $\Psi_w$ is given by the difference between the water influx from the veins ($J$, mol $m^{-2} s^{-1}$) and the water efflux from transpiration ($E$, mol $m^{-2} s^{-1}$) divided by the leaf capacitance ($C_{dyn}$, mol $m^{-2}$ $MPa^{-1}$):

$$\frac{d\Psi_w}{dt} = \frac{J - E}{C_{dyn}} \tag{2}$$

At a given moment, $\Psi_w$ can be found by knowing its previous value ($\Psi_{w,\ t-x}$) plus the integral of the differences between $J$ and $E$ during the desired period:

$$\Psi_{w(t)} = \Psi_{w,t-x} + \frac{\int_{t-x}^{t} [J(\tilde{t}) - E(\tilde{t})]\, d\tilde{t}}{C_{dyn}} \tag{3}$$

Here, $\Psi_w$ at the end of the VPD transition was measured ($\Psi_{w,\ final}$) and the previous changes in $\Psi_w$ ($\Psi_{w,\ t\text{-}x}$) were calculated every 10 s by approximating the integral of the differences between $J$ and $E$ during this period as

$$\int_{t-10s}^{t} [J(\tilde{t}) - E(\tilde{t})]\, d\tilde{t} \sim (J_{t-10s} - E_{t-10s})*10$$

resulting in our working formula:

$$\Psi_{w,t-10s} = \Psi_{w,\ final} - \frac{(J_{t-10s} - E_{t-10s})*10}{C_{dyn}} \tag{4}$$

where $J$ is the instantaneous flow rate into the leaf as measured by the flowmeter and normalized by projected leaf area and $E$ is the instantaneous flow rate out of the leaf as measured by the LiCor-6400. Our approach is similar to the one presented in Powles *et al.* (2006) who also inferred the $g_s$ dynamics from water balance in excised leaves; however, our method has the advantage of measuring the leaf hydraulic supply. As a result, it is possible to study not only the closure but also the kinetic of $g_s$ opening. The $\Psi_w$ reconstruction was made using Equation 4, beginning with the final $\Psi_w$ at the end of the data series and working backwards over $t$ seconds to the initial $\Psi_w$. Once all $\Psi_w$ values throughout the VPD transition were calculated, $K_L$ values were inferred from instantaneous flux ($E$) values and reconstructed instantaneous $\Psi_w$ values as

$$K_L = -E/\Psi_w \tag{5}$$

It is important to note that the dual flux $K_L$ calculated using Equation 5 presents characteristics of both current approaches to the measurement of $K_L$, the evaporative flux method (EFM) and the rehydration kinetics method (RKM) (Flexas *et al.* 2013). We believe that immediately after increasing VPD (i.e. at the moment of greatest divergence from steady-state), dual flux $K_L$ largely reflects the properties of water flow into dehydrated cells, thus being similar to the RKM method. On the other hand, as $g_s$ approaches steady-state, dual flux $K_L$ reflects flow along the normal steady-state transpiration stream, thus being similar to the EFM method. Thus, the inferred $K_L$ values here presented were obtained at the end of VPD phases, that is, immediately before the increase (first phase) and decrease (second phase) in VPD as it is believed these $K_L$ better reflect the hydraulic pathway of a naturally transpiring leaf (Buckley *et al.* 2015).

An important step for the $\Psi_w$ reconstructions was the assumption that the initial water supply rate from the xylem equals the steady-state leaf transpiration rate (as predicted by mass balance); thus, the LiCor-6400 and the flowmeter fluxes were matched just before the first step change in VPD. By doing this, we avoided small mismatches between the flowmeter and the LiCor that could produce an artefactual change in $\Psi_w$ and/or $K_L$.

### Half-times for stomatal closure and structural traits

Half-times for stomatal closure were estimated by fitting the time-course of $g_s$ closure (following a step change from low to high VPD) to an exponential decay model:

$$g_s(t) = g_{s\_high\ VPD} + \left(g_{s\_low\ VPD} - g_{s\_high\ VPD}\right) * e^{-k*t} \quad (6)$$

where $g_{s\_high\ VPD}$ is the steady-state $g_s$ at high VPD and $g_{s\_low\ VPD}$ is the steady-state $g_s$ at low VPD, $t$ is the time in seconds. The half-times, expressed in seconds, were calculated as $\ln(2)/k$. The rate constant, $k$, was fitted by non-linear fitting using the software Microsoft Excel. Briefly, the Excel's Solver Add-in was used to find $k$ as the value that minimizes the sum of squared differences between observed and predicted data. Initial estimates for $g_{s\_high\ VPD}$ and $g_{s\_low\ VPD}$ were the lowest and highest $g_s$ observed in the dataset. For $k$, the initial estimate was the inverse of the average from the estimates for $g_{s\_high\ VPD}$ and $g_{s\_low\ VPD}$.

Leaf mass per unit area (LMA) was calculated for six leaves sampled from each species (one leaf per individual), by dividing dry weight of harvested tissue by the projected leaf area. Tissue was dried at 70 °C for 72 h. The water content per unit leaf area (W, mol m$^{-2}$) was calculated for each species by calculating the difference between wet weight and dry weight, converting this mass to moles and dividing by the projected leaf area.

### Dynamic passive hydraulic model for stomatal conductance

The stepwise passive hydraulic model for $g_s$, described in Brodribb & McAdam (2011), successfully predicted the $g_s$ response to dehydration and VPD transitions in lycophytes, ferns and conifers (McAdam & Brodribb, 2014) given the hydraulic parameters ($K_L$ and $C_{dyn}$) and the $g_s$ and $\Psi_w$ function are known. Usually, this function is obtained from slowly desiccating leaves, but, alternatively, the dual flux technique allows its determination from attached leaves in a faster way. Thus, we tested whether the model, using the dual flux $g_s$ and $\Psi_w$ function, could predict the time-course of the $g_s$ response to changes in VPD in order to corroborate the passive hydraulic control by leaf hydration in the light.

The first step is to use a given value of $\Psi_w$ ($\Psi_{initial}$) to obtain $g_s$ as

$$g_s = f(\Psi_w) \quad (7)$$

Then, a transpiration value ($E$) can be calculated for a given VPD and atmospheric pressure ($P_{atm}$) as

$$E = g_s \mathrm{x}\ \mathrm{VPD}/P_{atm} \quad (8)$$

As $K_L$ is known, the steady-state $\Psi_w$ ($\Psi_{ss}$) for such $E$ would be

$$\Psi_{ss} = -E/K_L \quad (9)$$

Note that if $\Psi_{initial}$ and $\Psi_{ss}$ are identical, the $g_s$ value is under steady-state and no further changes in $\Psi_w$ will happen; however, if $\Psi_{initial}$ and $\Psi_{ss}$ are different, then a new $\Psi_w$ value ($\Psi_i$) will be calculated considering the buffering effect caused by $C_{dyn}$ for a time ($t$) of 1 s as

$$\Psi_i = \Psi_{ss} + (-\Psi_{ss} + \Psi_{initial}) \times e^{\frac{-tK_L}{C_{dyn}}} \quad (10)$$

Here, the model starts a new iterative cycle where $\Psi_i$ becomes $\Psi_{initial}$, and the cycling through Equations 7–10 starts again. Steady-state $g_s$ for a given VPD will be attained by calculating $\Psi_i$ through $n$ cycles (each cycle comprising 1 s) until $\Psi_{initial}$ and $\Psi_{ss}$ are identical. Note that, when this condition is achieved, the term ($\Psi_{ss} + \Psi_{initial}$) in Equation 10 is zero and the new $\Psi_i$ is equal to $\Psi_{ss}$. At any time, VPD transitions can be obtained by changing VPD in Equation 8. For the sake of simplicity, we assumed that changes in $K_L$ did not occur throughout the VPD transitions because $g_s$ returned to initial values after the transition from high to low VPD (Fig. 3). The $\Psi_{initial}$ and $K_L$ used to start the iterative process were those measured at the end of the VPD transitions. Average $C_{dyn}$ for each species was used, and we also modelled how the time-course of $g_s$ would be changed assuming a 50% change in $C_{dyn}$ to take into account possible individual differences in $C_{dyn}$. The dual flux $g_s$ and $\Psi_w$ relationships used In Equation 7 were linear functions and are presented in the Supporting Information.

## STATISTICS

Data are expressed as the means ± standard deviation. Student's $t$-tests were used to compare inferred $K_L$ between low and high VPD treatments. All statistical analyses were carried out using Microsoft Excel.

## RESULTS

The conifers and ferns studied here encompassed a substantial range in $K_L$, $C_{dyn}$ and W from 0.7 to 7.5 mmol m$^{-2}$ s$^{-1}$ MPa$^{-1}$, 150 to 2100 mmol m$^{-2}$ MPa$^{-1}$ and 5.6 to 36.8 mol m$^{-2}$, respectively (Table 1). Across species, neither $C_{dyn}$ nor $K_L$ were correlated with W or LMA. The half-times for the decrease in $g_s$ upon change in VPD were highly correlated with $C_{dyn}$ ($r = 0.96$, $P = 0.003$), less well correlated with $K_L$ ($r = 0.75$, $P = 0.09$) and not correlated with stomata length ($r = 0.32$, $P > 0.1$) indicating $C_{dyn}$ has a dominant influence on the speed of the stomatal response to VPD (Fig. 1). Indeed, the variability in $K_L$ and $C_{dyn}$ rendered half-times for stomata closures as fast as 89 s (*H. tenuifolia*) and as slow as 253 s (*C. rhomboidea*).

The wide range in $K_L$ and $C_{dyn}$ resulted in distinct patterns in the liquid and vapour fluxes into and out of the leaf (Fig. 2). After a transition from 1–2 kPa, high capacitance species such as *C. rhomboidea, M. glyptostroboides* and *P. lingua* presented increasing water deficits (higher vapour efflux than liquid influx) for up to 14 min, whereas in low capacitance species (*C. myriophylla, A. capillus-veneris* and *H. tenuifolia*) water deficit increased for periods as short as 4 min. All species showed a decrease in $g_s$ at increased VPD, but diverged in their

**Table 1.** Hydraulic and anatomical/morphological traits for the six sampled species. Leaf hydraulic conductance, $K_L$ (mmol $m^{-2}$ $s^{-1}$ $MPa^{-1}$); dynamic capacitance, $C_{dyn}$ (mmol $m^{-2}$ $MPa^{-1}$); half-times for stomata closure ($t_{1/2\_gs}$); water content, W (mol $m^{-2}$); leaf mass per unit leaf area, LMA (g $m^{-2}$); stomata length ($\mu$m). Values are averages ± standard deviation

| | $K_L$ | $C_{dyn}$ | $t_{1/2\_gs}$ | W | LMA | Stomata length |
|---|---|---|---|---|---|---|
| *Callitris rhomboidea* | 7.5 ± 0.29 | 2100 ± 62 | 253 ± 44 | 31.8 ± 6.2 | 202 ± 44 | 46 ± 2 |
| *Metasequoia glyptostroboides* | 4.1 ± 0.45 | 1022 ± 252 | 150 ± 36 | 13.1 ± 1.6 | 47 ± 11 | 22 ± 3 |
| *Pyrrosia lingua* | 0.7 ± 0.31 | 531 ± 26 | 177 ± 22 | 26.2 ± 2.5 | 142 ± 13 | 33 ± 2 |
| *Cheilanthes myriophylla* | 2.5 ± 0.39 | 347 ± 121 | 128 ± 13 | 8.0 ± 1.2 | 49 ± 8 | 38 ± 3 |
| *Adiantum capillus-veneris* | 2.1 ± 0.25 | 203 ± 92 | 91 ± 14 | 5.6 ± 0.5 | 25 ± 2 | 32 ± 3 |
| *Hypolepis tenuifolia* | 2.7 ± 0.14 | 150 ± 50 | 89 ± 13 | 6.0 ± 0.9 | 38 ± 8 | 42 ± 4 |

magnitude: *C. rhomboidea* had the largest decrease (*c.* 47%), whereas *C. myriophylla* had the lowest (*c.* 21%) (Fig. 3). No significant hysteresis in $g_s$ was observed upon returning to the initial VPD with at least 91% recovery of initial $g_s$ observed in all species and opening occurring in a symmetrical fashion to the dynamics of stomatal closure.

The leaf water potential reconstructions over the VPD transition showed increases and decreases according to exponential decay and rise functions (Fig. 3 and Supporting Information Fig. S2) and differed between species according to variability in their hydraulic properties. Species with a similar magnitude in the $g_s$ response to VPD yet with very different $K_L$ exhibited contrasting $\Psi_w$ reconstructions. As an example, the conifer *M. glyptostroboides* and fern *A. capillus-veneris* had a similar reduction in $g_s$ during the VPD transition yet *M. glyptostroboides* with a $K_L$ twice as high as the fern *A. capillus-veneris* had only minor changes (<0.1 MPa) in reconstructed $\Psi_w$ over the VPD transition, whereas reconstructed $\Psi_w$ in *A. capillus-veneris* dropped by more than 0.3 MPa. Regarding the $K_L$ estimations, only *H. tenuifolia* showed a significant $K_L$ decrease (31%) in response to high VPD (Fig. 4); however, this decline was reversible upon return to low VPD. No differences were observed between the measured and inferred $K_L$ at low VPD in any species.

We tested our observed $g_s$ data during the VPD transitions with the predictions for $g_s$ based on a passive hydraulic model. Using this model, we investigated the impact on predicted $g_s$ caused by changing $C_{dyn}$ while maintaining constant $K_L$ (Fig. 5). Good agreement was found between modelled and observed data for most species, except for *C. rhomboidea* and *H. tenuifolia*, which presented the largest deviations from the 1:1 line between observed and modelled $g_s$ (Supporting Information Fig. S3). This was somewhat expected for *H. tenuifolia* as we found decreases in $K_L$ under high VPD; as a result, the assumption of constant $K_L$ in the model could not be met (Fig. 4). Apart from *P. lingua*, the remaining species exhibited a bi-modal relationship where the $g_s$ decrease was slightly underestimated and the increase was similarly overestimated by the hydraulic model. This pattern was prominent in *C. rhomboidea* as even changes of ±50% in $C_{dyn}$ could not fit the observed data (Fig. 5).

## DISCUSSION

We developed a technique to perform real-time measurements of $\Psi_w$ by monitoring the balance between liquid and vapour fluxes into and out of leaves. This technique also allowed us to probe the predicted leaf hydraulic properties and $K_L$ dynamics in response to changes in VPD using a diverse sample of structurally different ferns and conifers.

### Stomatal responsiveness to vapour pressure deficit

Our dual flux measurements (Fig. 2) vividly showed how different leaf hydraulic architectures (e.g. changes in $K_L$ and $C_{dyn}$) led to distinct dynamics in the liquid and vapour fluxes through the leaf. It has long been recognized that there is a time lag between the onset of transpiration and the initiation of sap flow in the stems of trees (Schulze *et al*. 1985) where longer time lags reflect larger whole-tree capacitance (Meinzer *et al*. 2004). Such observations are in agreement with the cohesion theory predicting that the discharge of water storage tissues would generate a negative tension pulling water through the xylem (Nobel 1999). Here, we demonstrate that the same phenomenon occurs at the leaf level: increased transpiration driven by high VPD leads to a capacitive release of water from an internal storage compartment in the leaf followed by an immediate rise in the liquid flux of water into the leaf; in turn, recharge of the compartment occurred upon returning to low VPD. A similar result was shown by Powles *et al.* (2006) in *Photinia* × *fraseri* following air excision where immediate water loss from guard cells causes the initial $g_s$ response to be merely hydropassive. Interestingly, whereas whole-tree hydraulic architecture decouples canopy transpiration from stem flow for periods of up to 3 h (Philips *et al*. 1997), even in the highest capacitance leaves (a very thick-leaved fern), equilibration times were 10 min at most, evidencing a close coordination between liquid and vapour phases. The different $K_L$ and $C_{dyn}$ also significantly impacted stomata responsiveness as seen by the differences in stomata closure half-times (Table 1). The correlation between the observed and expected time constants ($C_{dyn}/K_L$) predicted by the passive model was close to the 1:1 line (Supporting Information Fig. S4), except for *P. lingua*, which seems to have a variable $C_{dyn}$ dependent on the rate of desiccation (McAdam & Brodribb, 2013). Most importantly, these half-times were highly correlated with $C_{dyn}$ (Fig. 1 and Table 1), which demonstrates the major role for this trait in stomata control across species. There was no relationship

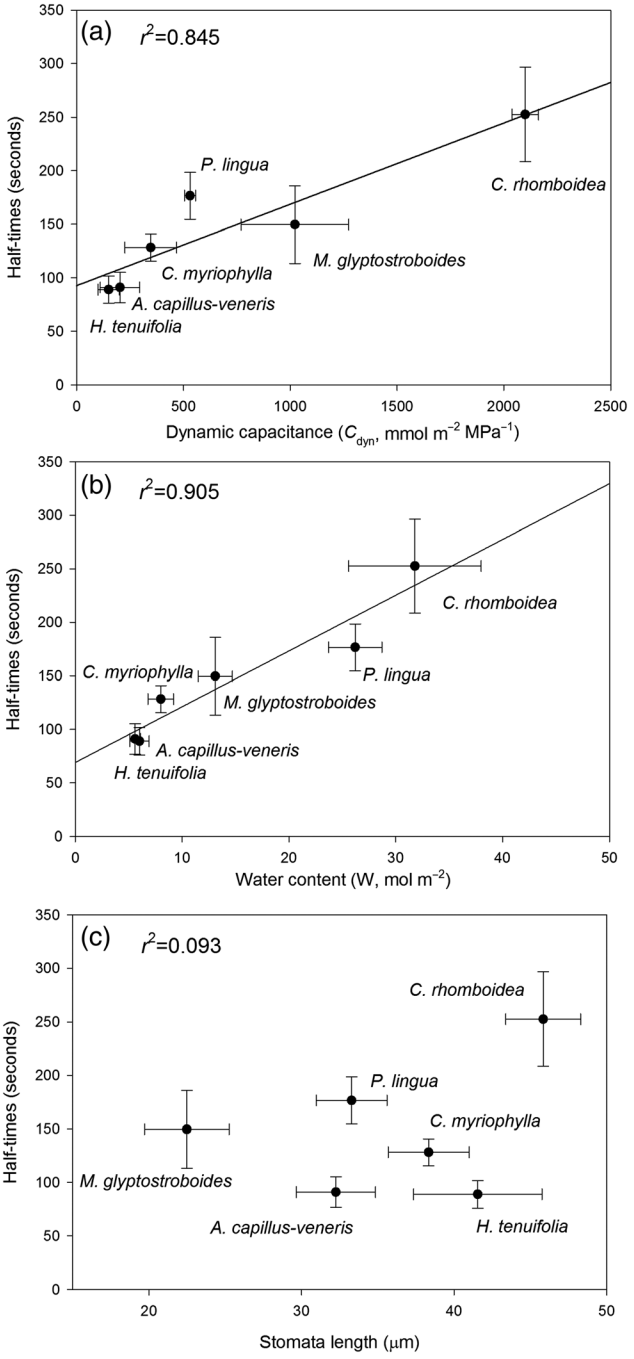


**Figure 1.** Plots showing the relationships between the half-times for stomata closure upon increase in vapour pressure deficit (VPD) from $1.0 \pm 0.1$ to $2.2 \pm 0.3$ kPa and (a) the dynamic capacitance ($C_{dyn}$, mmol m$^{-2}$ MPa$^{-1}$), (b) water content (W, mol m$^{-2}$) and (c) stomata length. Species with a higher $C_{dyn}$ or W tended to have longer half-times. Plotted values are averages ± standard deviation ($n = 3$).

between stomatal size and the speed of stomatal responses (Fig. 1), in contrast with recent reports suggesting stomatal size as a major determinant of response rates (Drake *et al.* 2013; Raven 2014). These conflicting results may indicate that, whereas leaf hydraulic architecture would dictate stomata response time in ferns and conifers where stomatal responses are passive (Brodribb & McAdam 2011), response speed would be presumably mediated by size-dependent metabolism (e.g. anion trafficking) in angiosperms.

## Leaf hydraulic conductance response to vapour pressure deficit

Despite the increasing number of studies reporting that $K_L$ can vary rapidly in response to factors such as leaf hydration, light, temperature, nutrient supply and ABA level (Scoffoni *et al.* 2008; but see Rockwell *et al.* 2011; Baazis *et al.* 2012; Lopez *et al.* 2013; Prado & Maurel 2013; Pantin *et al.* 2013), we did not find major changes in $K_L$ in response to VPD (Fig. 4). The only significant change in $K_L$ observed in any species was a reversible decrease (*c.* 30%) in *H. tenuifolia* under high VPD. Given the $g_s$ recovery to initial levels in this species, we discarded cavitation as the cause of reduced $K_L$ because it is highly unlikely that refilling would have occurred in such short time frame (Zwieniecki *et al.* 2013). Exposing *Piper auritum* leaves to high light and VPD caused similar reversible reductions in $K_L$ provided exposure to high light was not excessively long (Schultz & Matthews 1997). Besides cavitation, tracheid deformation (Zhang *et al.* 2014), leaf shrinkage and aquaporin deactivation (Scoffoni *et al.* 2014) could be able to cause reversible changes in $K_L$, but acting mostly on the outside-xylem component of $K_L$. In fact, *H. tenuifolia* had the second lowest LMA and W (Table 1) in addition to visually very fragile fronds thus producing a combination of traits that would make it very susceptible to leaf shrinkage. This possibility could be tested using anatomic studies of fronds exposed to low and high VPD to determine whether or not structural changes can have a role explaining these $K_L$ changes.

## Passive model of stomata control

In contrast to angiosperms, where stomatal responses to VPD are often characterized by hysteresis (McAdam & Brodribb 2015), we found that the stomata of our fern and conifer sample responded rapidly, symmetrically and according to the predictions of a hydropassive model in response to VPD (Fig. 5). This strongly supports a passive model of stomatal control in these taxa (Brodribb & McAdam 2011), while also demonstrating the impressive response speed that can be achieved by species where stomatal closure is independent of ABA-mediated signalling. Another pre-requisite for a passive hydraulic control is the direct effect of changes in leaf water content on guard cell turgor and, in turn, stomata aperture. Additionally, we implicitly assumed that the time constant for equilibration of guard cells relative to the bulk leaf would be negligible. This assumption seemed to be supported by our data for five out of the six species used in this study, which presented linear relationships between $g_s$ and $\Psi_w$ (Supporting Information Fig. S5). On the other hand, *C. rhomboidea*, the species with the largest $C_{dyn}$, showed a trend for $\Psi_w$ responding faster than $g_s$ to the VPD treatments causing its $g_s$ and $\Psi_w$ function to deviate from linearity (Supporting Information Fig. S5). The explanation for

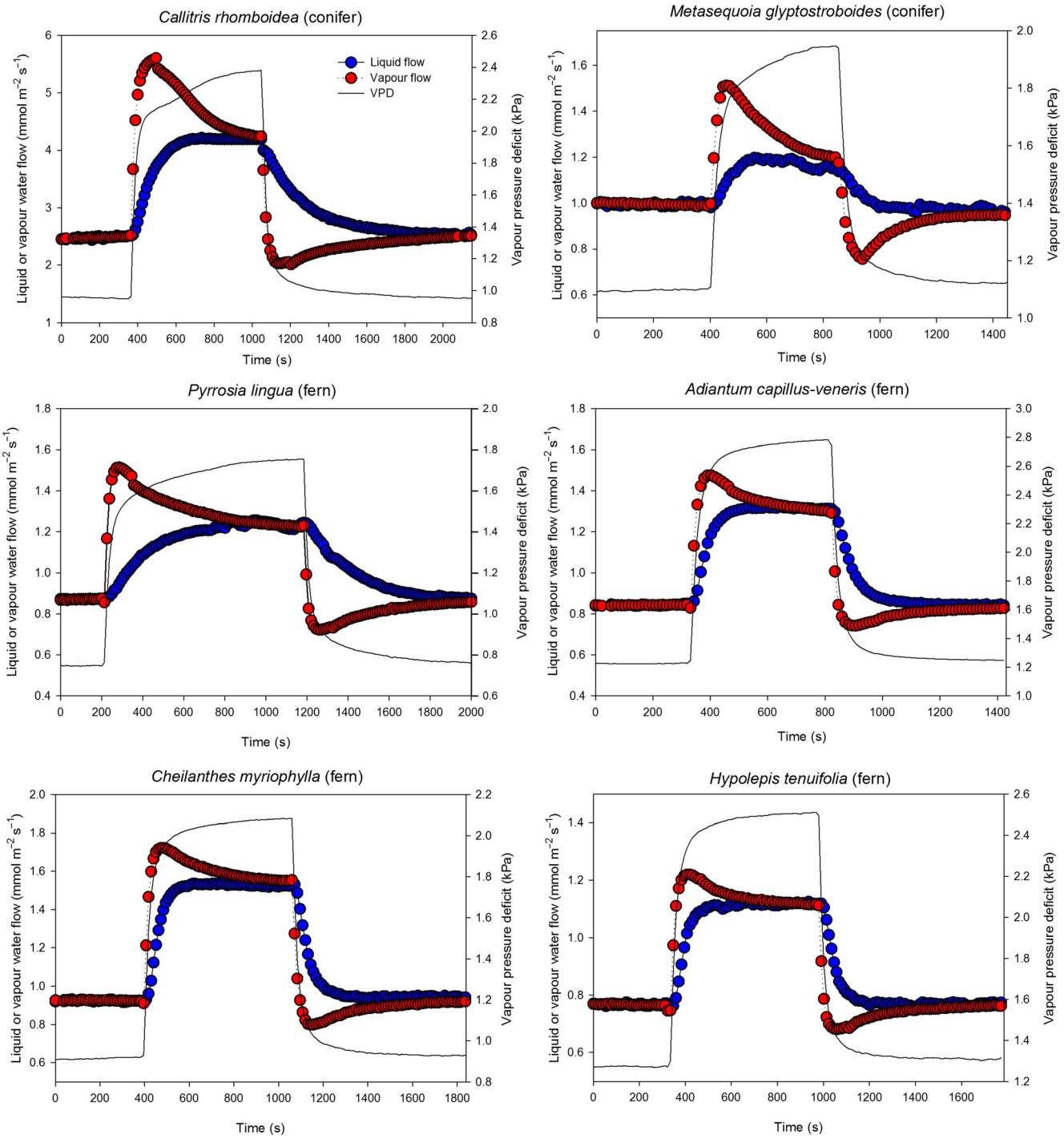


**Figure 2.** Dynamic changes in the fluxes of liquid and vapour phase water into and out of leaves. A representative individual of each species is shown. Solid lines show vapour pressure deficit (VPD), which was doubled and then returned to the initial value in two steps. The period when the vapour flux (red line) was higher than the liquid flux (blue line) corresponded to water deficit (leaf drying) and the opposite, liquid higher than vapour, water surplus meaning the leaf was rehydrating. Species with higher capacitance tended to have an extended period of deficit/surplus before reaching equilibrium. Note the difference in the fluxes scales to take into account the different magnitudes among species.

this may be the existence of a large resistor or capacitor between the leaf and the stomata acting as a kind of relay between the water status sensor and the guard-cells (Buckley, 2005). In any case, comparing leaves with similar large $C_{dyn}$ but contrasting leaf anatomy (presenting lignified mesophyll sclereids, for example) could help understanding how different leaf compartments affect the relationship between bulk $\Psi_w$ and $g_s$.

Regarding the changes in water content, we showed for the first time the extent to which water deficits developed *in situ*

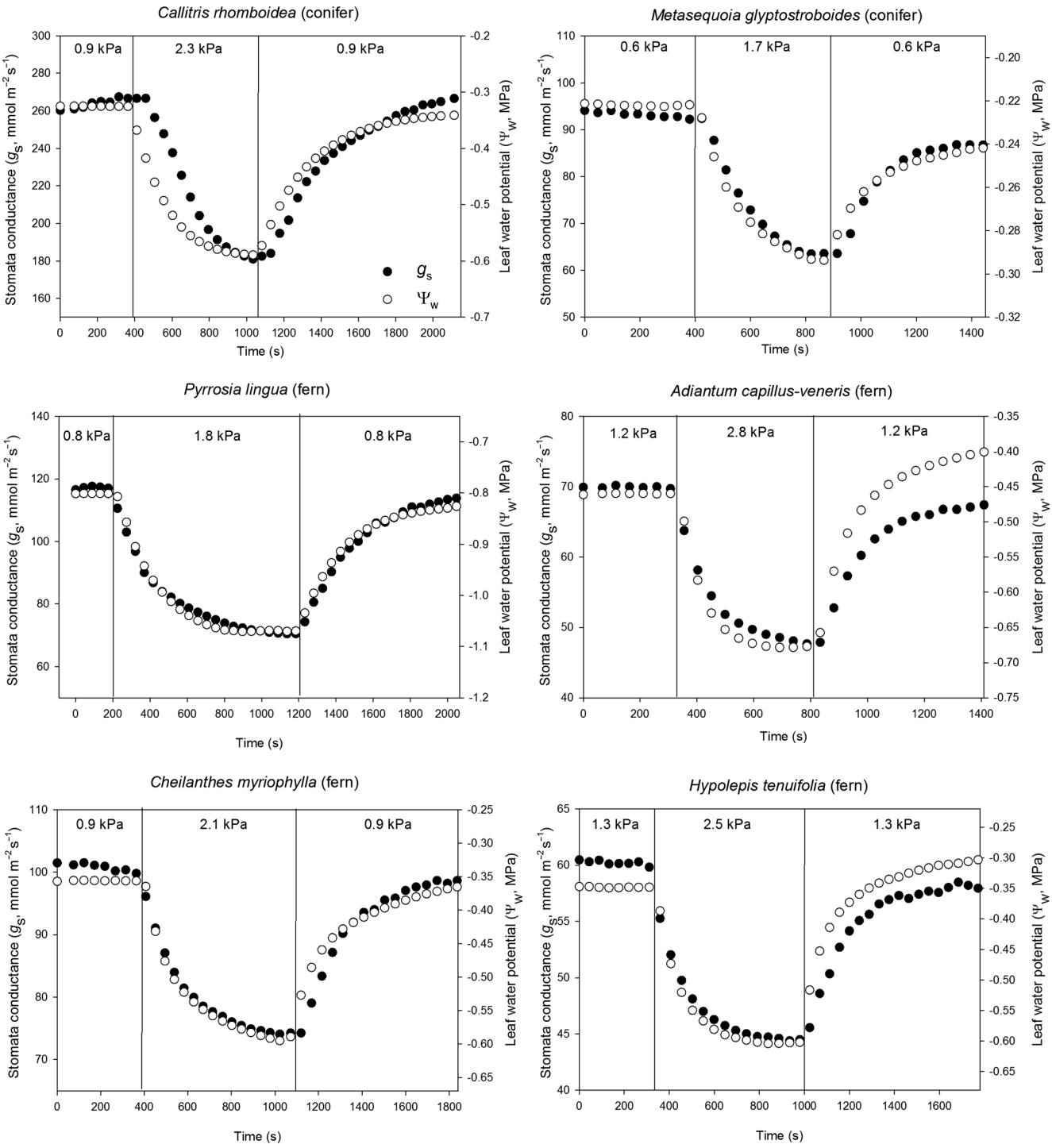


**Figure 3.** Stomatal conductance ($g_s$) and leaf water potential reconstructions ($\Psi_w$) based on water deficit calculations from liquid/vapour fluxes and capacitance. A representative individual of each species is shown. Vertical lines denote when vapour pressure deficit increased or decreased in a step change. The species were connected to a flowmeter supplying pure water, thus source water potential was *c.* 0 MPa.

during stomatal closure occur and how closely $g_s$ tracked these changes in $\Psi_w$. The deficits (*c.* 0.2–0.3 MPa, Fig. 3) were in the range known to cause substantial changes in $g_s$ in three out of four ferns here studied (McAdam & Brodribb 2013). Recently, the gymnosperm *M. glyptostroboides* was also shown to close passively in response to leaf water status under favourable water conditions and, actively (driven by ABA) when $\Psi_w$ approached turgor loss point (McAdam & Brodribb 2014). We found only minor changes in $\Psi_w$ (<0.1 MPa) during the VPD transition in *M. glyptostroboides* suggesting a steeper relationship between bulk $\Psi_w$ and $g_s$ in comparison to the other species here studied. As pointed out by Zwieniecki *et al.*

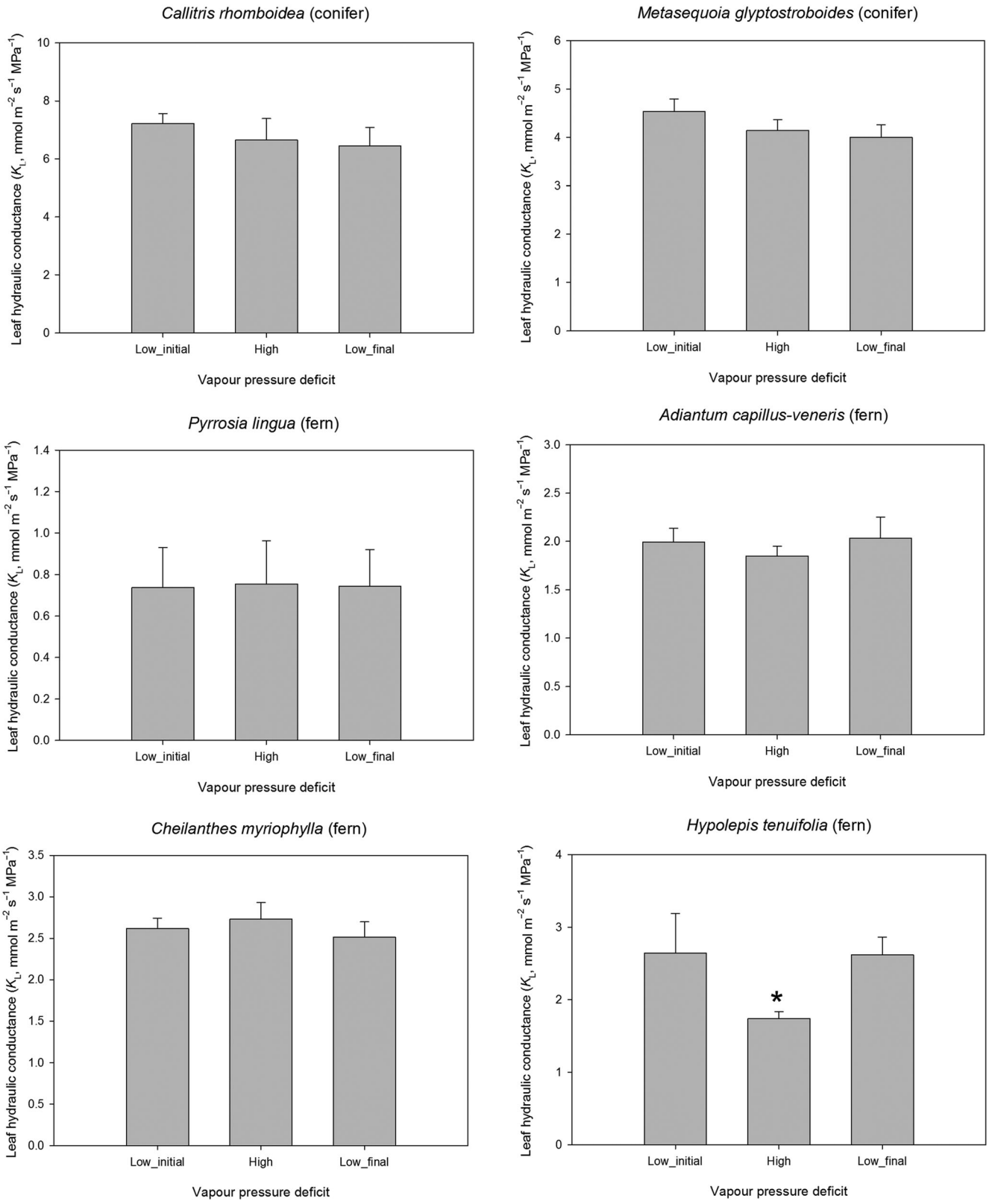


**Figure 4.** Leaf hydraulic conductance estimates ($K_L$) based on the dual flux technique as leaves were exposed to a reversible sequence of vapour pressure deficit (VPD) transitions from 1.0 ± 0.1 to 2.2 ± 0.3 kPa and returning to initial values. Plotted $K_L$ values were obtained at the end of each phase. An asterisk indicates statistically significant difference ($P < 0.05$) between low and high VPD treatments. Each bar is an average ± standard deviation from three individual per species.

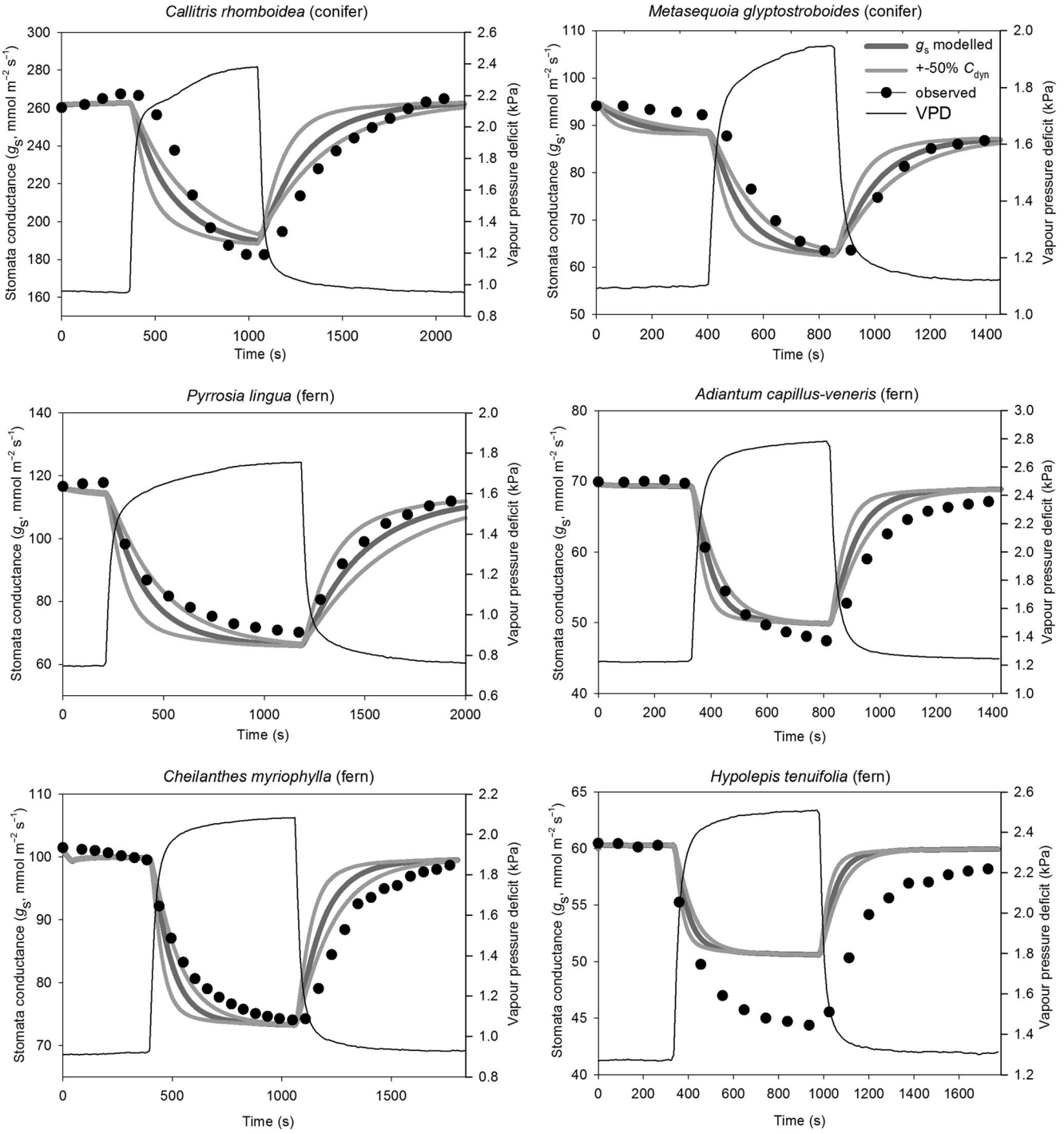


**Figure 5.** Examples of fitting the passive closure model to the observed stomatal dynamics. A single individual of each species is shown to facilitate comparison between observed and modelled data. In each case, dynamic behaviour of stomatal conductance ($g_s$) mirrored the behaviour of a passive hydraulic model (dark grey lines) using a constant leaf hydraulic conductance ($K_L$) as input. The passive model could not fit the observed $g_s$ in *Hypolepis tenuifolia* as this species presented a decrease in $K_L$ under high vapour pressure deficit (VPD) (Fig. 4), thus not meeting the assumption of constant $K_L$. A ±50% variation around the mean measured dynamic capacitance ($C_{dyn}$) is depicted as light grey lines. Note the differences in both scales in order to improve comparison between observed and modelled data.

(2007), it is possible that a relatively weak hydraulic connection between the vein and the rest of the leaf would result in a lower water potential at the epidermis, which is more likely to be influencing guard cell turgor. This was also suggested earlier by Buckley (2005) who observed stomata responding to changes in epidermal turgor that were too small to affect bulk $\Psi_w$. Hydraulic compartmentalisation could also decouple bulk $\Psi_w$ from the actual $\Psi_w$ driving changes in $g_s$; however, our $\Psi_w$ reconstructions were based on $C_{dyn}$, which is believed to more accurately represent the water fraction in tissues that readily

exchange water with the transpiration stream (Blackman & Brodribb 2011).

Despite the superior efficiency of angiosperm stomatal control in response to environmental factors related to photosynthetic signalling (e.g. light and $CO_2$) (McAdam & Brodribb 2012a; Brodribb & McAdam 2013), our data suggest that passive responses of stomata to VPD can provide a highly efficient control of water loss under variable VPD. Notably, this efficiency is mediated largely by the capacitance of the leaf. Thus, we predict that the stomata of most terrestrial rainforest ferns, many of which have low capacitances (McAdam & Brodribb 2013), should be very sensitive to changing VPD. This would provide highly effective protection in these moisture-sensitive species against tissue desiccation during diurnal fluctuations in VPD. It remains to be seen whether the dynamics of angiosperm stomata to changing VPD are also mediated by tissue capacitance. Because of the involvement of ABA in the response of angiosperm stomata to VPD (Bauer *et al* 2013; McAdam & Brodribb 2015), it might be expected that species-specific differences in the speed of metabolic processes involved in the synthesis and catabolism of ABA or the extrusion of ions may overwhelm the influence of physical traits such as leaf capacitance. Answering this question is not only critical for understanding the dynamics of angiosperm water use efficiency (WUE) but it would also provide a clearer target for breeders interested in modifying the WUE of angiosperm crops.

## CONCLUSION

We present a novel technique to measure online changes in $\Psi_w$ and $K_L$ allowing us to demonstrate the importance of hydraulic parameters in determining $g_s$ dynamics in response to VPD in ferns and conifers. Our data show that leaf hydraulics, mainly through changes in $C_{dyn}$, have a significant effect on the response time of stomata movements in ferns and conifers leading to closure rates as fast or faster than those seen in most angiosperms. We contend that the simple passive hydraulic control of stomata in response to changes in leaf water status provides an efficient stomata response to VPD, and it will be very interesting to investigate the extent to which hydraulic traits govern these responses in angiosperms, or whether such controls are largely overridden by metabolic control.

## ACKNOWLEDGMENTS

We thank the editor and two anonymous reviewers for their constructive and insightful comments. T.J.B. and S.A.M.M. received funding from the Australian Research Council (DP120101868, FT100100237 and DE140100946). S.C.V.M. was funded by a visiting scholarship to Tasmania from the Brazilian government CAPES/PDSE (6202/13-6). CNPq and Fapemig (fellowships to F.M.D.) are also greatly acknowledged.

## REFERENCES

Baaziz K.B., Lopez D., Rabot A., Combes D., Gousset A., Bouzid S., … Venisse J.S. (2012) Light-mediated *K*(leaf) induction and contribution of both the PIP1s and PIP2s aquaporins in five tree species: walnut (*Juglans regia*) case study. *Tree Physiology* **32**, 423–434.

Barman R., Jain A.K. & Liang M. (2014) Climate-driven uncertainties in modeling terrestrial gross primary production: a site level to global-scale analysis. *Global Change Biology* **20**, 1394–1411.

Bauer H., Ache P., Lautner S., Fromm J., Hartung W., Al-Rasheid K.A., … Hedrich R. (2013) The stomatal response to reduced relative humidity requires guard cell-autonomous ABA synthesis. *Current Biology* **23**, 53–57.

Blackman C.J. & Brodribb T.J. (2011) Two measures of leaf capacitance: insights into the water transport pathway and hydraulic conductance in leaves. *Functional Plant Biology* **38**, 118.

Brodribb T.J., Blackman C.J. (2011) Non-steady state rehydration to determine leaf hydraulic conductance, vulnerability and capacitance. *PrometheusWiki* (http://prometheuswiki.publish.csiro.au/tiki-index.php?page=Non-steady+state+rehydration+to+determine+leaf+hydraulic+conductance%2C+vulnerability+and+capacitance&highlight=capacitance).

Brodribb T.J. & Holbrook N.M. (2006) Declining hydraulic efficiency as transpiring leaves desiccate: two types of response. *Plant, Cell & Environment* **29**, 2205–2215.

Brodribb T.J. & McAdam S.A.M. (2011) Passive origins of stomatal control in vascular plants. *Science* **331**, 582–585.

Brodribb T.J., McAdam S.A.M. (2013) Unique responsiveness of angiosperm stomata to elevated $CO_2$ explained by calcium signalling. *PloS One* **8**, e82057.

Buckley T.N. (2005) The control of stomata by water balance. *New Phytologist* **168**, 275–292.

Buckley T.N., John G.P., Scoffoni C. & Sack L. (2015) How does leaf anatomy influence water transport outside the xylem? *Plant Physiology* **168**, 1616–1635.

Cramer W., Bondeau A., Woodward F.I., *et al.* (2001) Global response of terrestrial ecosystem structure and function to $CO_2$ and climate change: results from six dynamic global vegetation models. *Global Change Biology* **7**, 357–373.

Cowan L.R. & Farquhar G.D. (1977) Stomatal function in relation to leaf metabolism and environment. In *Integration of Activity in the Higher Plant* (ed Jenning D.H.), pp. 471–505. Cambridge University Press.

Damour G., Simonneau T., Cochard H. & Urban L. (2010) An overview of models of stomatal conductance at the leaf level. *Plant, Cell & Environment* **33**, 1419–1438.

Drake P.L., Froend R.H. & Franks P.J. (2013) Smaller, faster stomata: scaling of stomatal size, rate of response, and stomatal conductance. *Journal of Experimental Botany* **64**, 495–505.

Farquhar G.D., Lloyd J., Taylor J.A., Flanagan L.B., Syvertsen J.P., Hubick K.T., … Ehleringer J.R. (1993) Vegetation effects on the isotope composition of oxygen in atmospheric $CO_2$. *Nature* **365**, 368.

Flexas J., Scoffoni C., Gago J. & Sack L. (2013) Leaf mesophyll conductance and leaf hydraulic conductance: an introduction to their measurement and coordination. *Journal of Experimental Botany* **64**, 3965–3981.

Franks P.J. & Farquhar G.D. (2007) The mechanical diversity of stomata and its significance in gas-exchange control. *Plant Physiology* **143**, 78–87.

Hetherington A.M. & Woodward F.I. (2003) The role of stomata in sensing and driving environmental change. *Nature* **424**, 901–908.

Kim T.H., Bohmer M., Hu H., Nishimura N. & Schroeder J.I. (2010) Guard cell signal transduction network: advances in understanding abscisic acid, $CO_2$, and $Ca^{2+}$ signaling. *Annual Review of Plant Biology* **61**, 561–591.

Lange O.L., Losch R., Schulze E.-D. & Kappen L. (1971) Responses of stomata to changes in humidity. *Planta* **100**, 76–86.

Lawson T. & Blatt M.R. (2014) Stomatal size, speed, and responsiveness impact on photosynthesis and water use efficiency. *Plant Physiology* **164**, 1556–1570.

Lopez D., Venisse J.S., Fumanal B., Chaumont F., Guillot E., Daniels M.J., … Gousset-Dupont A. (2013) Aquaporins and leaf hydraulics: poplar sheds new light. *Plant & Cell Physiology* **54**, 1963–1975.

McAdam S.A.M. & Brodribb T.J. (2012a) Stomatal innovation and the rise of seed plants. *Ecology Letters* **15**, 1–8.

McAdam S.A.M. & Brodribb T.J. (2012b) Fern and lycophyte guard cells do not respond to endogenous abscisic acid. *Plant Cell* **24**, 1510–1521.

McAdam S.A.M. & Brodribb T.J. (2013) Ancestral stomatal control results in a canalization of fern and lycophyte adaptation to drought. *New Phytologist* **2**, 429–441.

McAdam S.A.M. & Brodribb T.J. (2014) Separating active and passive influences on stomatal control of transpiration. *Plant Physiology* **164**, 1578–1586.

McAdam S.A.M. & Brodribb T.J. (2015) The evolution of mechanisms driving the stomatal response to vapour pressure deficit. *Plant Physiology* **167**, 833–843.

Meinzer F.C., James S.A. & Goldstein G. (2004) Dynamics of transpiration, sap flow and use of stored water in tropical forest canopy trees. *Tree Physiology* **24**, 901–909.
Nobel P.S. (1999) *Physicochemical and Environmental Plant Physiology*. Academic Press, London.
Oren R., Sperry J.S., Katul G.G., Pataki D.E., Ewers F.W., Phillips N. & Schäfer K.V.R. (1999) Survey and synthesis of intra- and interspecific variation in stomatal sensitivity to vapour pressure deficit. *Plant, Cell & Environment* **22**, 1515–1526.
Pantin F., Renaud J., Barbier F., Vavasseur A., Le Thiec D., Rose C., … Simonneau T. (2013) Developmental priming of stomatal sensitivity to abscisic acid by leaf microclimate. *Current Biology* **23**, 1805–1811.
Peak D. & Mott K.A. (2011) A new, vapour-phase mechanism for stomatal responses to humidity and temperature. *Plant, Cell & Environment* **34**, 162–178.
Philips N., Nagchaudhuri A. & Oren R. (1997) Time constant for water transport in loblolly pine trees estimated from time series of evaporative demand and stem sap flow. *Trees* **11**, 412–419.
Prado K. & Maurel C. (2013) Regulation of leaf hydraulics: from molecular to whole plant levels. *Frontiers in Plant Science* **4**, 255.
Raven J.A. (2014) Speedy small stomata? *Journal of Experimental Botany* **65**, 1415–1424.
Rockwell F.E., Holbrook N.M. & Zwieniecki M.A. (2011) Hydraulic conductivity of red oak (*Quercus rubra* L.) leaf tissue does not respond to light. *Plant, Cell & Environment* **34**, 565–579.
Schultz H.R. & Matthews M. (1997) High vapour pressure exacerbates xylem cavitation and photoinhibition in shade-grown *Piper auritum* H.B. & K. during prolonged sunflecks. I. *Dynamics of water relations Oecologia* **110**, 312–319.
Schulze E.D., Cermák J., Matyssek R., Penka M., Zimmermann R., Vasícek F., … Kucera J. (1985) Canopy transpiration and water fluxes in the xylem of the trunk of *Larix* and *Picea* trees – a comparison of xylem flow, porometer and cuvette measurements. *Oecologia* **66**, 475–483.
Scoffoni C., Pou A., Aasamaa K. & Sack L. (2008) The rapid light response of leaf hydraulic conductance: new evidence from two experimental methods. *Plant, Cell & Environment* **31**, 1803–1812.
Scoffoni C., Vuong C., Diep S., Cochard H. & Sack L. (2014) Leaf shrinkage with dehydration: coordination with hydraulic vulnerability and drought tolerance. *Plant Physiology* **164**, 1772–1788.
Sellin A. & Lubenets K. (2010) Variation of transpiration within a canopy of silver birch: effect of canopy position and daily versus nightly water loss. *Ecohydrology* **3**, 467–477.
Simonin K.A., Burns E., Choat B., Barbour M.M., Dawson T.E. & Franks P.J. (2014) Increasing leaf hydraulic conductance with transpiration rate minimizes the water potential drawdown from stem to leaf. *Journal of Experimental Botany* . DOI:10.1093/jxb/eru481.
Tyree M.T. & Sperry J.S. (1988) Do woody plants operate near the point of catastrophic xylem dysfunction caused by dynamic water stress? *Plant Physiology* **88**, 574–580.
Zhang Y., Rockwell F.E., Wheeler J.K. & Holbrook N.M. (2014) Reversible deformation of transfusion tracheids in *Taxus baccata* is associated with a reversible decrease in leaf hydraulic conductance. *Plant Physiology* **165**, 1557–1565.
Zwieniecki M.A., Brodribb T.J. & Holbrook N.M. (2007) Hydraulic design of leaves: insights from rehydration kinetics. *Plant, Cell & Environment* **30**, 910–921.
Zwieniecki M.A., Melcher P.J. & Ahrens E.T. (2013) Analysis of spatial and temporal dynamics of xylem refilling in *Acer rubrum* L. using magnetic resonance imaging. *Frontiers in Plant Science* **4**, 265.

*Received 14 July 2015; received in revised form 16 October 2015; accepted for publication 18 October 2015*

## SUPPORTING INFORMATION

Additional Supporting Information may be found in the online version of this article at the publisher's web-site:

**Figure S1.** Examples of the gap-filling procedure used to estimate the missing stomatal conductance data ($g_s$). The missing $g_s$ for each VPD transition was filled (red dots) by fitting a model of an exponential decay through the remaining observed $g_s$ (blue dots) data and extrapolating back to the initial point where gs started to decrease (transition to high VPD) or increase (transition to low VPD).
**Figure S2.** Stomatal conductance ($g_s$) and leaf water potential reconstructions ($\Psi_w$) based on water deficit calculations from liquid/vapour fluxes and capacitance. Two additional individuals of each species are shown. Vertical lines denote when vapour pressure deficit as increased or decreased in a step change. The species were connected to a flowmeter supplying pure water, thus source water potential was *c.* 0 MPa.
**Figure S3.** Comparison between modelled and observed stomatal conductance ($g_s$). Modelled $g_s$ before and after step changes in VPD showed very close agreement with predictions from a passive hydraulic model of stomatal control in four fern and two conifers species. Except for *Callitris rhomboidea* and *Hypolepis tenuifolia*, the remaining species showed minor deviations from the 1:1 relationship between observed and modelled $g_s$.
**Figure S4.** Comparison between modelled ($C_{dyn}/K_L$) and observed time constants. Modelled time constants were calculated using measured values of leaf capacitance ($C_{dyn}$) and leaf hydraulic conductance ($K_L$). Observed time constants were obtained by fitting the time-course of stomatal closure (following a step change from low to high VPD) to an exponential decay model. Plotted values are averages ± standard deviation (n=3).
**Figure S5.** Stomatal conductance ($g_s$) and leaf water potential ($\Psi_w$) relationships as measured by the dual-flux technique. These relationships were used in the hydropassive model to generate the modelled $g_s$ time-course in response to VPD presented in Figure 5 and Figure S3.